Ind. J. Pharm. Edu. Res., 2024; 58(2s):s640-s647.
https://www.ijper.org

Original Article

Biogenic Synthesis of Copper Oxide Nanoparticle from *Aegle marmelos* and its Anti-Cancerous Potential against HCT-116 Cell Line

Nizar A. Khamjan[1], Abdullah Farasani[1, 2,*]

[1]Department of Medical Laboratories Technology, Faculty of Applied Medical Sciences, Jazan University, Jazan, SAUDI ARABIA.
[2]Biomedical Research Unit, Medical Research Center, Jazan University, Jazan, SAUDI ARABIA.

ABSTRACT

Background and Aim: Colorectal cancer stands as a frequently occurring fatal disease for several decades and the use of nanoparticles has long been explored in cancer treatments. Engineering the size and shape to attain an optimal efficacy of the nanoparticles and using a specific plant resource to enhance its compatibility to other healthy cell is a propitious approach. The present study investigates the anti-cancer activity of CuO NP synthesized from *Aegle marmelos* leaf extract against human colorectal cancer. **Materials and Methods:** The CuO NPs (Nanoparticles) exhibited promising characteristics with UV and SEM-EDAX, its photochemical constituents were analyzed with FTIR, and the geometry of the synthesized nano-particles was studied using Zeta potential and particle size analyzer. The cell viability was scrutinized via trypan blue assay and further toxicity was determined by cell morphology and several *in vitro* analyses where the MTT assay presented that the 25 µg/mL of CuO NPs as the IC_{50} concentration. **RESULTS:** The nuclear fragmentation was studied by DAPI staining which resulted in increased fluorescence of the treated cells indicating the robust effect of the CuO NPs and the mitochondrial damage was monitored through MMP analysis with declining fluorescence. The most vital aspect of understanding cancer pathogenesis is oxidative stress which was evaluated by ROS, NO, and LPO with favorable outcome. **Conclusion:** The cell viability and ROS assay coalesce to suggest that CuO NPs indeed induce apoptosis and it is evident that Biogenically synthesized CuO NPs contain anti-proliferative potential and promotes apoptosis.

Keywords: Colorectal cancer, *Aegle marmelos*, Nanoparticles, Copper Oxide, Anti-cancer.

Correspondence:
Dr. Abdullah Farasani
Biomedical Research Unit, Medical Research Center, Jazan University, Jazan-45142, SAUDI ARABIA.
Email: aofarasani@jazanu.edu.sa

Received: 18-09-2023;
Revised: 08-11-2023;
Accepted: 12-12-2023.

INTRODUCTION

Colorectal cancer is considered the most prevalent cancer type globally next to breast and cervical cancer. The pursuit of eradicating solid tumors in colorectal cancer using chemo and radiotherapy often results in recurrence and dose-limiting side effects, especially in the advanced stages. The side effects are due to the dampening of homeostasis resulting in susceptibility to infections, anemia, fatigue, and neurotoxicity.[1,2] To overcome these limitations, Nanoparticles (NPs) are being used, it is cost-effective and doesn't affect normal cells or induce drug resistance in cancer cells. The altered dimension of NPs enhances its interactive properties due to the surface-to-volume ratio which has shifted the limelight toward their anti-cancerous potential.

The Biocompatible nature of Metal-Oxide nanoparticle reportedly has more anti-proliferative capacity and interacts with macromolecules and promotes pro-inflammatory response.[3] The particle exposures of CuO NPs bring forth oxidative stress implying efficient bioavailability and it is way cheaper than most other NPs. However, the effect of this metal oxide NP needs a thorough study. Conventional chemical or physical methods need large-scale production facilities and use stabilizing and reducing agents, CuO NPs produced in this way have shown adverse health effects. Considerate to the environment as well as to limit the side-effects in humans, green synthesis is employed to produce CuO nanoparticle. Bacteria, fungi, algae, and plants can be used as a resource for green synthesis. Moreover, it can be more efficient, specific and cost-effective which well aligns with the current requirement in cancer treatments. The simplified downstream processing and instant retrieval of the nanoparticle as a final product without the need for separation and purification make it an ideal method. Compounds from plant resources make the NPs easily metabolized when administered as a drug compared to synthetically derived particles. The size and shape of the NPs can be easily engineered using plant-based synthesis,

DOI: 10.5530/ijper.58.2s.68

it is also the best way to eliminate the use of toxic materials for nanoparticle production and limit the production of harmful by-products. In this study plant resource is used as it is a one-pot extraction procedure thus reducing contaminants and providing sustainable synthesis.

Besides, metabolites like phenolic compounds, polysaccharides, enzymes, and certain functional groups including the amino group, carboxylic acid naturally acts as stabilizing and reducing agent. We utilized *Aegle marmelos*, generally called "bael" which is a plant of high medicinal value and it is known to cure diabetes, asthma, hypertension, dysentery, and inflammation. To the best of our knowledge, there are only limited studies of CuO NPs for their anti-cancerous property against Human colorectal cancer. So, given its high level of Phyto-constituent here we have characterized our CuO NPs with UV, FTIR, and SEM-EDAX, Zeta-potential and analyzed its cytotoxic potential by MTT, Trypan Blue, NO, LPO and ROS.

MATERIALS AND METHODS

Chemicals and Plant Material

All the chemicals used throughout the process are from Hi-Media. Fresh and disease-free *Aegle marmelos* (AM) leaves were collected and weighed to 20 g.

Synthesis of CuO NPs

The following procedure for the Synthesis of CuO NPs were slightly modified from previous studies.[4,5] The *Aegle marmelos* leaves were washed and finely chopped to immerse in 100 mL of dil. H–O and subjected to boiling at 80°C for 30 min. The boiled solution was filtered using Whatman No.1 filter paper. 100 mL of 10 mM copper chloride was prepared and added to the 20 mL of the prepared plant extract and kept for stirring at 80°C overnight. This was sonicated for 8 hr for further size reduction and purified by centrifugation at 10,000 RPM for 10 min at room temperature. Finally, the pellets were collected and dried overnight in a hot air oven forming a black-colored powder which is stored in a vacuum desiccator.

Characterization of Synthesized CuO NPs

UV-Visible spectroscopy was used to confirm the presence of the CuO NPs between the wavelength of 200-800 nm).[4] The composition of functional groups presents in the synthesized CuO NPs, FTIR was performed which can denote the compounds responsible for the reduction and capping of nanoparticles to their stability within the range of 400-4000[2] SEM-EDAX reveals the morphology of the NPs through the secondary electron images along with the presence of elemental Cu combined with other components.[6] The average size and stability were determined using zeta potential and the size distribution of particles is estimated using a particle size analyzer.

Cytotoxicity assay

A mitochondrial enzyme-dependent reaction is employed here, MTT (3-(4,5-dimethylthiazed-2-11)-2,5-diphenyl tetrazolium bromide) was dissolved in PBS (pH: 7.3) to obtain a concentration of 5 mg/mL. 10 µL of MTT was added into 96 well plates with cells treated with different concentrations of samples (0.1-100 µg/mL). The plate was incubated at 37°C, humidity as 5% CO_2 with 95% air for 4 hr. The reacted media is then aspirated and 150 µL of DMSO 0.5% (v/v) was added to dissolve the formed formazan crystals and the wavelength is absorbed at 560 nm.[7]

$$\% \text{ Viability} = \text{Absorbance of treated cells/Absorbance of Untreated} \times 100\%$$

Cell viability

Cell viability is determined using a trypan blue exclusion assay to estimate the extent of the cytotoxic effect of the CuO NPs (AM). The cells were grown in a T25 flask and harvested by trypsinization. This was centrifuged and transferred into 6 well plates and treated with the CuO NPs of 12.5 µg/mL, 25 µg/mL, and 50 µg/mL concentrations for 48 hr. The following day, the sample was discarded and incubated with 40 µL of 4% trypan blue for 5 min at 37°C. Then DMEM (Dulbecco's Minimum Eagle's Medium) was added to stop the reaction and cells were counted using a hemocytometer.[8]

$$\%\text{Viability} = \text{Number of viable cells/Total number of cells} \times 100$$

Morphological Analysis

Morphological disorientation imposed on HCT-116 cancer cells by the CuO NPs was compared with the control. 2×10^5 cells/well were seeded in 24 well plates with fresh DMEM medium and incubated for 48 hr with CuO NPs at IC_{50} concentration. Then the media was washed and taken for observation using a phase contrast microscope.[9]

MMP (Δψm)

The mitochondrial membrane potential was determined using lipophilic cation dye (Rhodamine 123). Mitochondrial damage is a significant indicator of apoptosis occurring at the IC_{50} concentration of the sample. 5×10^5 cells/well were seeded in 6 well plates and incubated overnight. These cells were treated with CuO NPs of varying concentrations. After 36 hr the media was removed and it was stained with 50 µL of rhodamine-123 (10 µg/mL) for 30 min. Excess dye was removed using PBS and the images were captured using a fluorescence microscope (Bio-Rad, Hercules, CA).[10]

DAPI

The morphology of the nucleus is studied using 4'6-Diamidina-2-Phenylindole (DAPI). After the culturing, the monolayered cells were washed with PBS and fixed using 3%

formaldehyde for 15 min at room temperature and permeabilized with 0.1% triton X-100 for 10 min. A concentration of 0.5 µg/mL DAPI was stained on the prepared cells and incubated for 10 min in the dark at 37°C. Then the cells were washed using PBS and visualized using a fluorescence microscope (Bio-Rad, Hercules, CA) at the excitation wavelength of 330-380 nm and emission wavelength of 430-460 nm.[9]

ROS

The intracellular reactive oxygen species is determined using an NBT assay. CuO NPs with DMEM and 0.2% NBT prepared in PBS are added to the seeded cells in 96 well plates and incubated for 1 hr at 37°C 5% CO_2 in the dark. After the incubation 0.1M HCL is added to stop the reaction and the cells were harvested after centrifugation at 1500 g for 10 min. DMSO was added to the pellets to extract the NBT. Finally, the formazan blue is detected at an absorbance of 575 nm.[11]

LPO

The oxidation of lipids is detected by measuring the produced secondary product MDA (Malondialdehyde). The cells were seeded at 2.0×10^5 cells per well in 96 well for 24 hr. The next day, it is treated with the NPs (12.5 µg/mL, 25 µg/mL, 50 µg/mL) and incubated for 48 hr. These CuO NPs treated cells were harvested and washed twice using ice-cold PBS; the cells were collected and subjected to disruption using mortar and pestle with KCL Buffer (pH 6) for 5 min. The extract collected (10% w/w) with a reaction mixture of 8.1% SDS, 1.5mL of 20% acetic buffer (pH 3.5), and 1.5 mL of 0.8% aqueous thiobarbituric acid was heated at 95°C for 60 min. This mixture was allowed to cool and then combined with 5 mL of (15:1) n-butanol pyridine and shaken vigorously to obtain the appearance of a red pigmentation. This is centrifuged and the organic layer is taken for estimation at 532 nm against the standard of tetra methoxy propane.[12,13]

NO

Radical scavenging activity is estimated using Griess reagent. First the 2×10^5 cells/well were seeded in the 96 well plates with CuO NPs of different concentrations and incubated for 24 hr with fresh DMEM media. The next day, the media was collected and an equal amount of Griess reagent is added to 1 mL of this incubated media and left in the dark at room temperature to react and estimated using a UV spectrometer at 550nm.[2]

RESULTS

UV-vis Spectrophotometry

The color change from yellow to brown was observed which indicated the formation of CuO NPs. Further, the surface Plasmon resonance observed through UV-visible spectrum using Cary 60 (Agilent, CA, the US) of the synthesized nanoparticles present in the extract are excited and showed a prominent peak at 225 nm wavelength at an absorbance of 0.188 confirming the presence of CuO in the sample (Figure 1).

Fourier Transform Infrared Radiation

The FTIR read a broad range of regions from 400-4000 cm^{-1} to cover most of the functional groups. (Figure 2a and b) In the AM plant extract, there is a broad peak observed at 3248.55cm-1 corresponds to OH stretching due to the phenol group present and the sharp peak at 1581 cm^{-1}, 1397cm^{-1}, 1068 cm^{-1} shows the NH bending of primary amines, CN of aromatic nitro group and COOH of carboxylic acid respectively. The presence of fingerprint region in NPs synthesized with AM extract shows the involvement of the AM plant extract in CuO stability. A broad peak can be seen in CuO synthesized extract akin to the phenol peak of AM plant extract. Additionally, other sharp peaks can be observed at 2334 cm^{-1}, 2174 cm^{-1}, 1591 cm^{-1} of NH stretching and 1055 cm^{-1} corresponding to the ester functional group.[4,5]

Scanning Electron Microscope-Electron Dispersive X-rays analysis

The electron image of surface topography and morphological analysis of CuO NPs is interpreted using SEM (Oxford Instruments, Abingdon, England). Figure 3 reveals that the nano-particles are in irregular quadrilateral shapes and are equally distributed among the space. From the EDAX results it is seen that the Cu constituent is in the majority of about 53.4% and O of 23.1% representing the abundance of CuO NPs in the sample.

Zeta potential

At a temperature of 25°C and viscosity of dispersion medium as 0.894 mPa, the particle size of the NPs dispersed was noted. As observed from the Figure 4 the zeta potential is -43.9 mV and the electrophoretic mobility was -0.000340 cm^2/Vs which assures that the NP produced are stable compounds, this is interpreted using HORIBA SZ-100 (Horiba, Kyoto, Japan) for Windows [Z Type] Ver2.00.

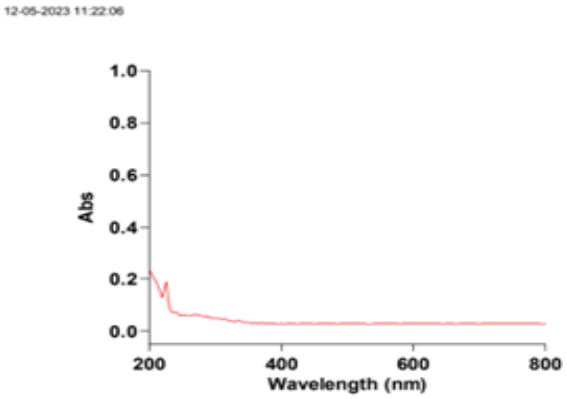

Figure 1: UV-vis spectra of CuO Nanoparticle.

Particle size analyzer

The particle size analyzer (HORIBA SZ-100Kyoto, Japan) estimated the average size of the CuO NPs as 21.7 nm in a mono-dispersed condition. The scattered light intensity is represented in the Figure 5, at the temperature and medium viscosity of 25°C and 0.894 mP as respectively. This suggest that the CuO NPs synthesized are of appropriate size.

Cytotoxicity assay

The metabolically collapsed cells with disrupted mitochondria in the HCT116 cell line was subjected to an MTT assay to analyze the cytotoxicity of NPs with varying concentration. Upon the addition of DMSO after incubation, MTT added to the wells turned purple with descending color intensity with increasing dosage of CuO NPs considered as a primary observation. The quantitative data is depicted in Figure 6, when compared to the control the results display a spike in inhibition at the highest concentration of 50 µg/mL indicating the anti-cancerous effect of the CuO NPs respective to their dosage. It is conspicuous that the concentration of 25 µg/mL holds the IC_{50} range.

Cell viability

We studied the cell viability with Trypan blue exclusion assay and the Figure represents that there is a sequential plunge in cell viability compared to control with the increase in the concentration of CuO NPs. Results show higher significance with treated cells of almost 100% cell viability and this decline to around 13% with 12.5 µg/mL concentration and increases to 44% at 25 µg/mL compared to the control. The final concentration of 50 µg/mL subsides to a 63% of drop-in viability supporting the anti-proliferative effect of AM synthesized CuO NPs (Figure 7).

Morphological analysis

The treatment of HCT 116 cells with varying concentration of 12 µg/mL, 25 µg/mL and 50 µg/mL caused the detachment of treated cells from the flask after 48 hr. At 20X magnification, distinct morphological changes like membrane blebbing, shrinkage caused by the nano-particle was visualized.

DAPI

DAPI is a non-toxic stain compatible with other chromogen and it does not disorient the ultra-structure of the cell presenting a reliable interpretation. From Figure 8 it is clear that the intensity of the fluorescence escalates steadily with increasing concentration whereas the nuclear fluorescence was prominently diminished in control cells.

MMP

The intensity of green fluorescence decreases with an increase in CuO concentration. The Figure 9 distinctly exhibits the drastic drop in the membrane potential with higher dosage. It is noted that the fluorescence is almost completely deprived in 50 µg/mL and only traceable fluorescence is found at 25 µg/mL concentration compared to the image of the control cells.

ROS

The effect of CuO NPs is majorly decided by the enhanced amount of ROS as it represents its potential killing activity which is determined using NBT. The reduction of NBT by the superoxide generated from the CuO NPs is quantitatively estimated by ROS (Reactive oxygen species). Results are expressed as mean and SD, the treated cells showed high significance compared to the control (p<0.0001). From the Figure 10, the ROS level of the treated cells with the highest dosage has increased to 76% in contrast to the control cells.

LPO

The anti-oxidative action of CuO NPs has increased and the treated cells showed high significance compared to the control cells (p<0.0001). From the Figure 11 it is evident that there is a dose dependent increase in lipid peroxidase level and the results

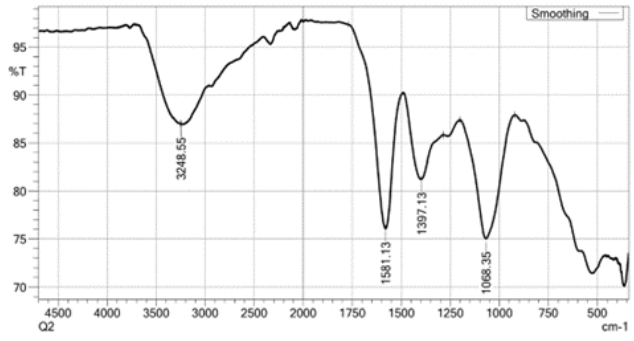

Figure 2: a) FTIR Spectra of *Aegle marmelos* leaf extract. b) FTIR Spectra of CuO Nano-particle synthesized using *Aegle marmelos* leaf extract.

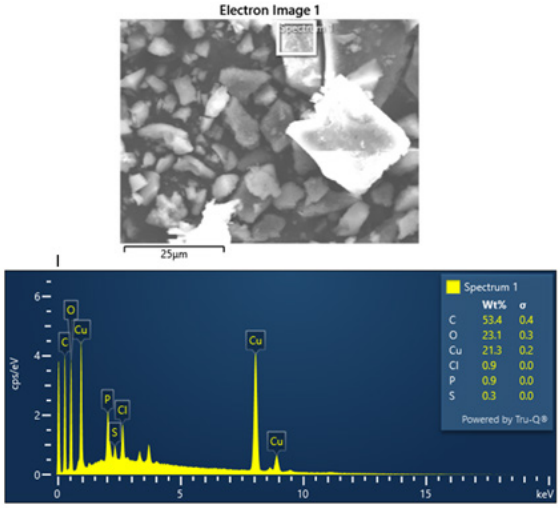

Figure 3: a) SEM analysis indicating the size, shape and distribution of CuO NPs. b) EDAX analysis of chemical constituens of the CuO NPs synthesized.

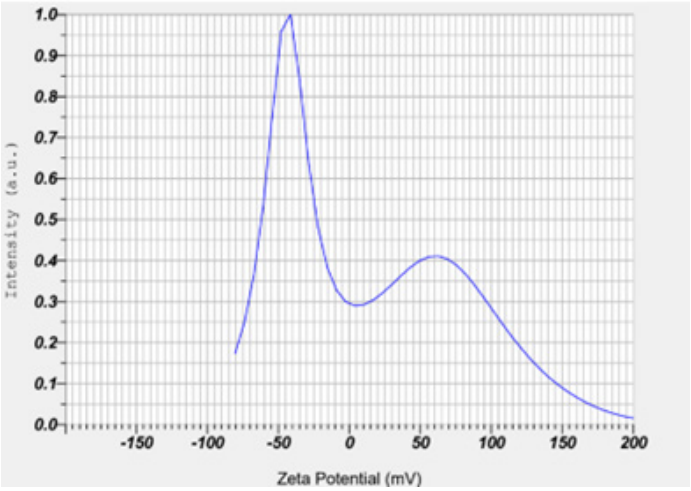

Figure 4: Zeta potential of the synthesized CuO NPs.

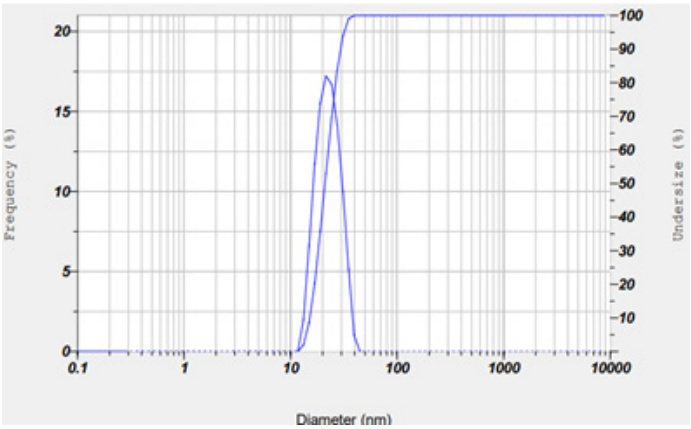

Figure 5: Particle size analyzer of the synthesize CuO NPs.

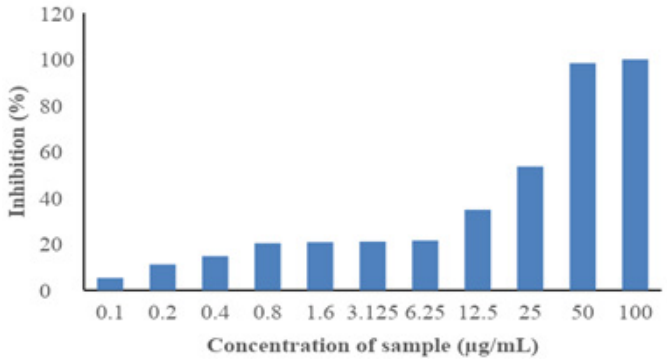

Figure 6: Cytotoxicity of the treated cells are estimated in MTT Assay.

are subjected to one-way ANOVA (Tukey multiple comparison test) analysis and showed a significant difference between control and treated cells. There is a drastic improvement of 16% from 12.5 µg/mL concentration to 25 µg/mL and 35% improvement in contrast to the control. Whereas there is a notable increase of 9% when the concentration is upscaled from 25 µg/mL to 50 µg/mL and 43% compared to the control. This shows the effectiveness of the CuO NPs against human colorectal cancer with increasing dosage.

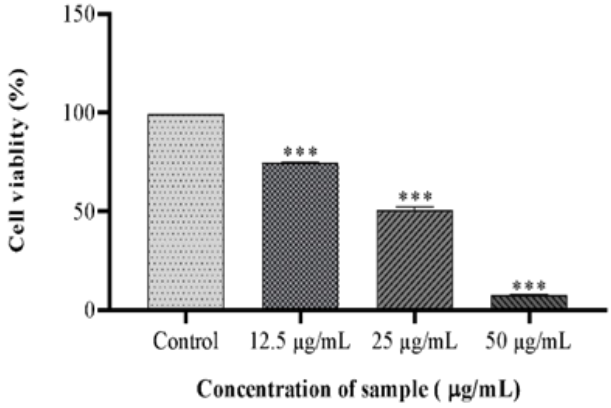

Figure 7: Extent of cell viability of control and CuO NPs treated cells are measured by Trypan Blue Exclusion Assay.

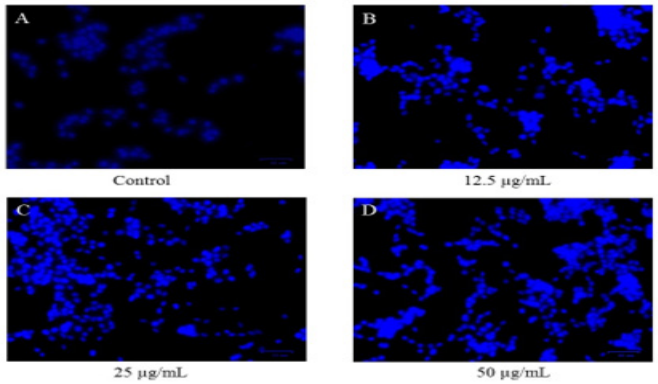

Figure 8: Nuclear morphology by DAPI staining using fluorescence microscopy at a magnification of 10X of the control and the treated cells.

NO

The generated NO radical forms chromophore with Griess reagent and it was measured at 550 nm. The NO concentration has progressively increased due to the cell damage caused by improved concentration of NPs Figure 12 indicates the level of NO with increased nanoparticle concentration, denoting the antagonistic capability of the CuO NPs. It is observed that the concentration of 12.5 µg/mL and 25µg/mL has an average of 2.3% to 2.7% NO level respectively and a sustained increase of 0.83% and 1.3% respectively when compared to the control. Ultimately, 2.1% increase is observed in the highest dosage of 50 µg/mL compared to the control and exhibiting a 3.77% of total NO level.

DISCUSSION

Nanoparticles have physicochemical properties through their size and shape which make them chemically more reactive in possessing biological activities that can be either desirable in drug delivery or by inducing oxidative stress.[14] This makes it important to assess their characteristic for their promising cytotoxic effect. The color change of the plant extract during

the synthesis proves the generation of CuO NPs. Besides, the UV spectra further confirmed the presence of CuO NPs with a peak at 225 nm. The SEM images and zeta analysis reconfirmed their appropriate sizes, though contrast to other earlier studies.[2] The CuO NPs are in uneven quadrilateral shapes. Furthermore, this unique and homogeneously distributed dimension may be due to the use of *Aegle marmelos* specifically for this biogenic synthesis. However, SEM analysis concurs an even distribution of the nanoparticle which could be caused majorly by the capping and stabilization of phenolic compounds present in the plant extract. The stability based on the intermolecular interaction within the NP molecules and with the aqueous medium was estimated through zeta potential. The zeta potential values of -43.9 mV obtained showed the stability of the CuO NPs, as the higher the negative value more the stability of NPs, this resulted in no repulsion or agglomeration of the NPs.[15] The FTIR confirms the presence of a phenolic compound which is synchronous to the peaks observed at 3355 cm^{-1} from a previous study on CuO NPs synthesized from *A. marmelos*.[16] The cytotoxic effect of CuO NPs in *Aegle marmelos* (AM) has not been extensively studied especially in the human colorectal cancer treatments against the synthesis of CuO NPs using various other plants. Reports from[4] show that the IC_{50} is attained at high concentration whereas CuO NPs obtained from AM plant is highly potent even at much lower concentration, this indicates the enhanced efficiency of the synthesized CuO NPs using *A. marmelos*. Based on Tabrez *et al.*, 2022[16] where the IC_{50} is at 25 µg/mL concentration from pumpkin seeds similar to the CuO NPs synthesized from AM leave extract proves its equal efficiency. The morphology study viewed in a phase-contrast microscope is coherent with the observation by similar works with cell shrinkage, cytoplasmic membrane blebbing, and damaged cells into small membranes were observed in treated cells due to the cell rupture caused by CuO NPs.[9,16] This is because the concentration of CuO NPs accumulates inside the cells and the structural integrity is disrupted. Further, DAPI staining determined the changes in the nucleus as a consequence of apoptosis. Mitotic cells possess distinct round nuclei and are not fragmented as apoptotic cells, which has caused the intense and bright stain with DAPI, this helped to understand the nuclear morphological changes and proved the apoptotic potential of

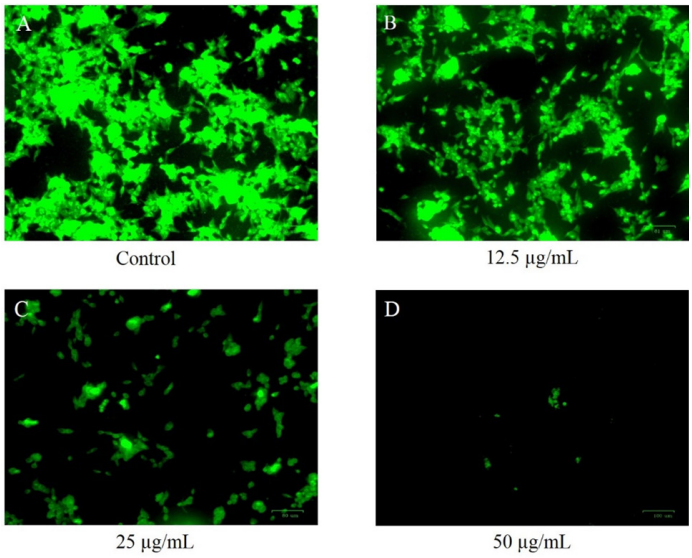

Figure 9: Mitochondrial membrane potential of the control cells and the treated cells with the synthesized CuO NPs.

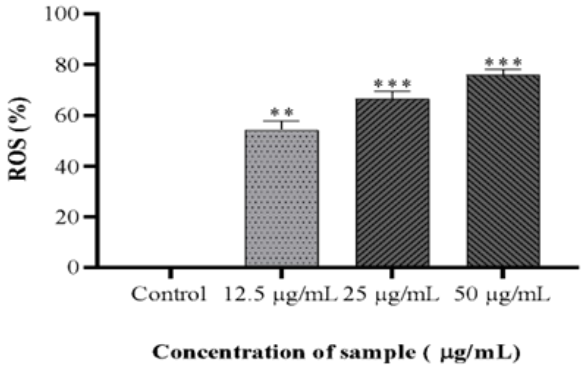

Figure 10: Potential killing activity of CuO NPs is determined using NBT with control cells in Reactive Oxygen Species (ROS) Assay.

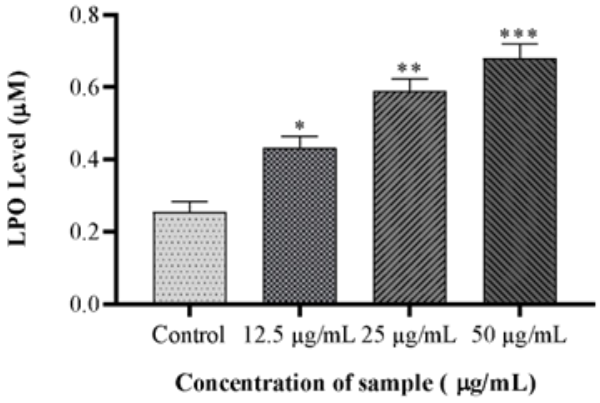

Figure 11: Anti-oxidative potential of CuO NPs is estimated in Lipid Peroxidation (LPO) Assay.

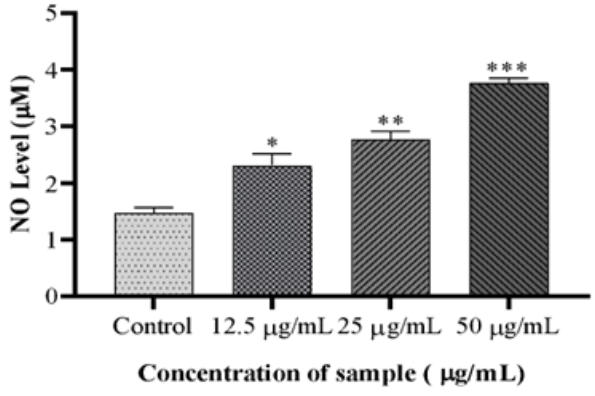

Figure 12: The concentration of NO radical is evaluated with Nitric Oxide (NO) Assay.

the CuO NPs.[8,9] DAPI bound to A-T rich region of DNA by electrostatic interaction stops the internal rotation which causes the consistent fluorescence in treated cells.[17] Intact cells showed bright-colored areas of non-condensed chromatin in the nucleus but the necrotic cells having condensed chromatin exhibited a dull fluorescence.[14] Results showed that morphological identification of apoptosis and apoptotic DNA fragmentation occurred as a consequence of CuO NPs. Mitochondrial damage is a significant indicator of the cytotoxic effect caused by NPs on HCT-116. Here, post-treatment with IC_{50} concentration of CuO NP the mobility of cytochrome C to the cytosol indicates the apoptotic stage induced by CuO NP, the cell damage caused by CuO NPs paved the way for the Rhodamine123 to bind with the mitochondrial membrane causing the orange color to green color appearance. This cationic dye adhered to the matrix concerning the electric potential across the mitochondrial membrane which according to few studies could lead to caspase-dependent apoptosis.[10,18] Less vital cells express less fluorescence produced by the dye indicating the energized ($\Delta\psi m$) intact mitochondria. Involving in this intrinsic pathway Rodamine-123 expressed weak fluorescence conveying a decreased MMP after CuO NPs treatment.[19]

Occurrence of oxidative stress is an essential phenomenon in cancer pathogenesis and it happens when there is an imbalance in the ROS and anti-oxidant homeostasis. Production of ROS has a particular mechanism with different NPs depending on their surface, size, composition and the presence of metal. Although the mechanisms are undefined these intrinsic factors cause cell damage by deposition of NP in cellular and sub-cellular surfaces. Apoptosis is the main form of cell death induced by NP dependent oxidative stress.[20] As a cancer antagonist, CuO NPs induced the pro-apoptotic gene and pro-apoptotic protein p21 and down-regulate the cell cycle regulatory protein by producing ROS.[18] This was evident in the NBT assay where the NBT is reduced with the superoxide generated by the cells exposed to CuO NPs and the magnitude of ROS generated was maximum at the highest CuO NPs concentration of treated cells. This is due to the free radical which is bound to the NPs reacting with the oxygen, resulting in ROS production triggering apoptosis-mediated receptors and damaged mitochondria.[20] Free radical-induced damage of polyunsaturated fatty acids disrupts cellular bio-membrane and causes lipid peroxidation. In the LPO assay, the damaged HCT 116 cellular membrane releasing free radicals produced by LPO is a reliable sensitive marker for cellular toxicity and here the abundance of LPO is exposed by the derivative Malondialdehyde (MDA) reacting to Thiobarbituric Acid (TBA), this conciliates the effectiveness of CuO NPs as an anti-cancer drug.[21,11] Though the CuO NPs synthesized using Azadirachta indica leaves have been reported to have increased levels of NO in the MCF-7 and HeLa cells Dey *et al*., 2019[22] and many research with similar effects with other plant extracts on different cell lines exists, the elevated NO index has not been emphasized in cytotoxicity studies of CuO NPs using *Aegle marmelos* in HCT-116 cell line. Nevertheless, from the NO assay performed in this study we perceive that the Nitrative stress has surged in the cells treated with 50 µg/mL of CuO NP concentration. The NO induces pro-inflammatory response and acts as a signaling molecule in pathogenesis causing DNA damage and cell injury by the CuO NP exposure.[23] By far the synthesized CuO NP has shown to be effective even in minimal concentration with the aid of stability provided by AM extract. Thus, this can account for the biogenic synthesis of CuO NPs to be a promising drug for human colorectal cancer. Moreover, optimizing the anti-proliferative effects of the nanoparticle specified only to the cancer cells but compatible and nurturing towards healthy cells could hold the potential to unravel the CuO NPs into playing a double-edge sword in the administration of targeted treatments. This holistically ensures the safety and efficacy of both diagnostics and treatment of colorectal cancer.

CONCLUSION

We studied the CuO NP's promising characteristics and its effect on HCT-116 cell line also its efficient internalization into these cells. In this discourse, various cellular assays like MTT, cell viability, NO, LPO, DAPI provided the NPs with an ample support on its prolific anti-cancerous potential. Therefore, the successful one-pot Biogenic synthesis of CuO NPs with the aid of the phytochemicals present in *Aegle marmelos* marks it as an effective candidate for colon cancer treatment as a novel drug therapy.

ACKNOWLEDGEMENT

The authors extend their appreciation to the Deanship of Scientific Research, Jazan University, for supporting this research work through the Wa'ed Research Program (number W41-049).

CONFLICT OF INTEREST

The authors declare that there is no conflict of interest.

ABBREVIATIONS

MTT: 3-(4,5-dimethylthiazol-2-yl)-2,5-diphenyltetrazolium bromide; **ROS:** Reactive Oxygen Species; **EDTA:** Ethylenediamine tetra acetic acid; **PBS:** Phosphate buffered saline; **FBS:** Fetal Bovine Serum; **DMSO:** *Dimethyl sulfoxide;* **DMEM:** Dulbecco's Modified Eagle Medium; **MMP:** Mitochondrial Membrane Potential; **LPO:** Lipid peroxidation; **NO:** Nitric oxide.

SUMMARY

- The current study intended to evaluate CuO NPs from *Aegle marmelos* leaf extract for antiproliferative effect on HCT-116 cells.

- The MTT assay revealed that cytotoxicity increased in a dose-dependent manner. The LC_{50} range was determined to be 25 mg/mL concentration.
- Cells shrinkage, cell detachment and membrane blebbing were observed in synthesised CuO NPs treated cells, indicating antiproliferative activity.
- The health of mitochondria can be determined by their membrane potential. Increased ROS can cause membrane potential to collapse, which can cause apoptosis.
- On treating the HCT-116 cells with nanoparticles, the oxidative stress enzymes such as Reactive oxygen species, Lipid peroxidation, and Nitric oxide were significantly elevated.
- Overall, synthesised CuO NPs from *Aegle marmelos* treated HCT-116 cells enhances the anti-cancer and antioxidant activity by scavenging the free radicals.

REFERENCES

1. Anuradha G, Manimekalai R. Antibacterial activity of green synthesized copper sulphate doped gold Nano particles from the leaf extract of *Aegle marmelos* L. *~891 ~ Journal of Pharmacognosy and Phytochemistry*. Vol. 8(4); 2019.
2. Jayakodi S, Shanmugam VK. Statistical optimization of copper oxide nanoparticles using response surface methodology and Box-Behnken design towards *in vitro* and *in vivo* toxicity assessment. Biointerface Res Appl Chem. 2021; 11(3): 10027-39. doi: 10.33263/BRIAC113.1002710039.
3. Khan S, Ansari AA, Khan AA, Abdulla M, Al-Obaid O, Ahmad R. *In vitro* evaluation of cytotoxicity, possible alteration of apoptotic regulatory proteins, and antibacterial activity of synthesized copper oxide nanoparticles. Colloids Surf B Biointerfaces. 2017; 153: 320-6. doi: 10.1016/J.COLSURFB.2017.03.005, PMID 28285257.
4. Gnanavel V, Palanichamy V, Roopan SM. Biosynthesis and characterization of copper oxide nanoparticles and its anticancer activity on human colon cancer cell lines (HCT-116). J Photochem Photobiol B. 2017; 171: 133-8. doi: 10.1016/J.JPHOTOBIOL.2017.05.001, PMID 28501691.
5. Kulkarni V, Kulkarni P. Synthesis of copper nanoparticles with *Aegle marmelos* leaf extract. Nanosci Nanotechnol. 2014; 8: 401-4.
6. Nagajyothi PC, Muthuraman P, Sreekanth TVM, Kim DH, Shim J. Green synthesis: *in vitro* anticancer activity of copper oxide nanoparticles against human cervical carcinoma cells. Arab J Chem. 2017; 10(2): 215-25. doi: 10.1016/j.arabjc.2016.01.011.
7. Mosmann T. Rapid colorimetric assay for cellular growth and survival: application to proliferation and cytotoxicity assays. J Immunol Methods. 1983; 65(1-2): 55-63. doi: 10.1016/0022-1759(83)90303-4, PMID 6606682.
8. Sreelatha S, Jeyachitra A, Padma PR. Antiproliferation and induction of apoptosis by *Moringa oleifera* leaf extract on human cancer cells. Food Chem Toxicol. 2011; 49(6): 1270-5. doi: 10.1016/j.fct.2011.03.006, PMID 21385597.
9. Choudhary A, Elumalai P, Raghunandhakumar S, Lakshmi T, Roy A. Anti-Cancer Effects of *Saraca asoca* flower extract on Prostate Cancer Cell Line. J Pharm Res Int. 2021: 330-8. doi: 10.9734/jpri/2021/v33i62B35621.
10. Baracca A, Sgarbi G, Solaini G, Lenaz G. Rhodamine 123 as a probe of mitochondrial membrane potential: evaluation of proton flux through F0 during ATP synthesis. Biochim Biophys Acta Bioenerg. 2003; 1606(1-3): 137-46. doi: 10.1016/S0005-2728(03)00110-5.
11. Valodkar M, Jadeja RN, Thounaojam MC, Devkar RV, Thakore S. Biocompatible synthesis of peptide capped copper nanoparticles and their biological effect on tumor cells. Mater Chem Phys. 2011; 128(1-2): 83-9. doi: 10.1016/j.matchemphys.2011.02.039.
12. Gasparovic AC, Jaganjac M, Mihaljevic B, Sunjic SB, Zarkovic N. Assays for the measurement of lipid peroxidation. Methods Mol Biol. 2013; 965: 283-96. doi: 10.1007/978-1-62703-239-1_19, PMID 23296666.
13. Ohkawa H, Ohishi N, Yagi K. Assay for lipid peroxides in animal tissues by thiobarbituric acid reaction. Anal Biochem. 1979; 95(2): 351-8. doi: 10.1016/0003-2697(79)90738-3, PMID 36810.
14. Rahmani Kukia N, Abbasi A, Maysam S, Froushani A. Copper oxide nanoparticles stimulate cytotoxicity and apoptosis in glial cancer cell Line; 2018.
15. Yugandhar P, Vasavi T, Uma Maheswari Devi P, Savithramma N. Bioinspired green synthesis of copper oxide nanoparticles from *Syzygium alternifolium* (wt.) Walp: characterization and evaluation of its synergistic antimicrobial and anticancer activity. Appl Nanosci. 2017; 7(7): 417-27. doi: 10.1007/s13204-017-0584-9.
16. Tabrez S, Khan AU, Mirza AA, Suhail M, Jabir NR, Zughaibi TA, *et al.* Biosynthesis of copper oxide nanoparticles and its therapeutic efficacy against colon cancer. Nanotechnol Rev. 2022; 11(1): 1322-31. doi: 10.1515/ntrev-2022-0081.
17. Spinale, F.G., and Nicholson, J. H. 1991. DAPI as a useful stain for nuclear quantitation.
18. Manikandan R, Beulaja M, Arulvasu C, Sellamuthu S, Dinesh D, Prabhu D, *et al.* Synergistic anticancer activity of curcumin and catechin: an *in vitro* study using human cancer cell lines. Microsc Res Tech. 2012; 75(2): 112-6. doi: 10.1002/jemt.21032, PMID 21780253.
19. Bai Aswathanarayan J, Rai Vittal R, Muddegowda U. Anticancer activity of metal nanoparticles and their peptide conjugates against human colon adenorectal carcinoma cells. Artif Cells Nanomed Biotechnol. 2018; 46(7): 1444-51. doi: 10.1080/21691401.2017.1373655, PMID 28884587.
20. Manke A, Wang L, Rojanasakul Y. Mechanisms of nanoparticle-induced oxidative stress and toxicity. BioMed Res Int. 2013; 2013: 942916. doi: 10.1155/2013/942916, PMID 24027766.
21. Rabiee N, Bagherzadeh M, Kiani M, Ghadiri AM, Etessamifar F, Jaberizadeh AH, *et al.* Biosynthesis of copper oxide nanoparticles with potential biomedical applications. Int J Nanomedicine. 2020; 15: 3983-99. https://doi.org/10.2147/IJN.S255398doi: 10.2147/IJN.S255398, PMID 32606660.
22. Dey A, Manna S, Chattopadhyay S, Mondal D, Chattopadhyay D, Raj A, *Azadirachta indica* leaves mediated green synthesized copper oxide nanoparticles induce apoptosis through activation of TNF-α and caspases signaling pathway against cancer cells. Journal of Saudi Chemical Society. 2019; 23(2): 222-38. https://doi.org/10.1016/j.jscs.2018.06.011doi: 10.1016/j.jscs.2018.06.011.
23. Park EJ, Park K. Oxidative stress and pro-inflammatory responses induced by silica nanoparticles *in vivo* and *in vitro*. Toxicology Letters. 2009; 184(1): 18-25. https://doi.org/10.1016/j.toxlet.2008.10.012doi: 10.1016/j.toxlet.2008.10.012, PMID 19022359.

Cite this article: Khamjan NA, Farasani A. Biogenic Synthesis of Copper Oxide Nanoparticle from *Aegle marmelos* and its Anti-Cancerous Potential against HCT-116 Cell Line. Indian J of Pharmaceutical Education and Research. 2024;58(2s):s640-s647.